Enhanced Knowledge in Sciences and Technology Vol. 3 No. 2 (2023) 292-301

EKST

Homepage: http://publisher.uthm.edu.my/periodicals/index.php/ekst
e-ISSN : 2773-6385

Analysis of the Corrosion Products of the External X70 Pipeline: Sea and River Water Environment

Siti Hazirah Johari[1], Zaidi Embong[1*], Khawarizmi Mohd Jafery[1]

[1]Department of Physics and Chemistry,
Faculty of Applied Sciences and Technology
Universiti Tun Hussein Onn Malaysia (Pagoh Campus),
84600 Pagoh, Muar, Johor, MALAYSIA

*Corresponding Author Designation

DOI: https://doi.org/10.30880/ekst.2023.03.02.035
Received 16 January 2023; Accepted 15 February 2023; Available online 30 November 2023

Abstract: Pipeline corrosion can degrade pipeline surfaces, cause leaks, and endanger oil and gas workers. The characterization of the oxide layer formed on external X70 steels, as well as understanding its formation mechanisms, are critical factors in the development and improvement of materials' corrosion resistance. This study investigated the corrosion products of X70 pipeline steel for pre- and post-immersion in seawater of Pontian, Johor, and river water of Panchor River, Johor. The pH and salinity values of sea and river water were measured using a pH meter and Refractometer, respectively. The corrosion rates of steels were determined using the mass loss method after immersion for 7, 14, and 21 days. The surface morphology and composition of their corrosion product were characterized using DSX100 Opto-Digital Microscope, X-ray Diffraction (XRD), Field Emission Scanning Electron Microscope (FESEM), and Scanning Electron Microscopy with Energy Dispersive X-ray (SEM-EDX). The pH values were 7.2 and 6.3, respectively, and the salinity of seawater was 22.0 ppt, and that of river water was 0.4 ppt. The average mass loss of X70 steels immersed in sea and river water for 7, 14, and 21 days was 0.1097 g and 0.0610 g, respectively. The average corrosion rate of those steels in river water was 3.1954 g/cm^{2}h, while that in seawater was 1.7470 g/cm^{2}h. Subsequently, elemental analysis by EDX indicated that the corrosion products consist of Fe (98.3%) and Si (1.63%) for pre-immersion, while for post-immersion in seawater were Fe (74.54%), O (24.04%), and Cl (1.35%), and in river water were Fe (74.44%), O (24.08%), and Cl (0.10%). Overall, the corrosion products observed were lepidocrocite (γ-FeOOH), goethite (α-FeOOH), hematite (Fe_2O_3), magnetite (Fe_3O_4), and akageneite (β-FeOOH) as revealed by FESEM, SEM and XRD analysis.

Keywords: X70 Pipeline Steel, Seawater, River Water, XRD, FESEM, SEM-EDX

**Corresponding author: zaidi@uthm.edu.my*

1. Introduction

Oil and gas are vital resources that account for more than half of the users of the world's energy today. The oil and gas industry is currently experiencing increased demand and is unaffected by the transition to clean energy. Both oil and gas are transported from one location to another via pipelines [1]. X70 pipeline steels are regulated according to the American Petroleum Institute's (API) standard 5L, and the design considerations outlined in API-5L are based on alloy chemistry and tensile strength. The chemical compositions of X70 are mainly C, Mn, S, P, and other elements such as Cr, V, and Nb [2].

Additionally, pipelines that are made from steel are buried in various environments, including marine environments, which have several variables that may contribute to the corrosion of the pipeline exterior surface [3]. Therefore, there are varieties of research proposed about the mechanism of steel in the marine environment with multiple parameters such as chloride attack, microbiology-induced corrosion, sulfide attack, oxygen level, pH level, acidity, salinity, and more [4].

Correspondingly, corrosion is an ordinary process for metal since all natural processes tend toward the lowest possible energy states. For instance, steel and iron have a natural tendency to combine with other chemical elements like oxygen and water by adsorption of the gas on the surface to return to their lowest energy states which form hydrated iron oxides (rust) [5]. In the oil and gas industry, surface degradation and material failure of pipelines have a significant impact, resulting in massive losses for the industry because of increased maintenance spending. It is a consequence of leakage, holes, and gouges on the external surface of pipelines that may induce harm to the environment and humans, as well as disrupt the process of petroleum transfer [4]. In this context, a study of surface characterization of corrosion products is crucial to provide further explanation of the X70 pipeline corrosion induction mechanism. This is achieved by performing several analyses such as XRD, FESEM and Scanning Electron Microscopy with Energy Dispersive X-Ray (SEM-EDX) with a special emphasis on surface morphological characterization of the corrosion products on the external of the X70 pipeline after being immersed in seawater and river water for various period which was 7, 14, and 21 days.

2. Materials and Methods

2.1 Sample Preparation

The X70 steel was cut into seven pieces with the dimensions of 10 mm ×10 mm × 3 mm using Mitsubishi EDM Wire Cut Machine and polished using 800 grit paper to remove deformed surface material. Then, X70 steel was stored in a container filled with silica gel to remove moisture. The sample of seawater was taken within Tambak Pontian, Johor, while the sample of river water was taken at Sungai Panchor, Johor, as shown in Figure 1. Each piece of X70 steel was immersed in 50 ml amount of sea and river water in a closed beaker for 7, 14, and 21 days.

(a) (b)

Figure 1: The location of water sample collection (a) seawater (b) river water.

2.2 Sample Characterization

Prior to external surface characterization, pH monitoring for seawater and river water needs to be carried out. For this purpose, the pH of each water sample was measured using a Milwaukee pH meter, while the salinity of each water sample was recorded using a Refractometer. For the post-immersion process, the mass of each coupon was weighed accurately to quantify its mass loss and corrosion rate. Meanwhile, the chemical and physical characterization for both pre and post-immersed samples is performed using several analytical techniques, including DSX100 Opto-Digital Microscope XRD, FESEM, and SEM-EDX.

3. Results and Discussion

3.1 Physical and Chemical Properties of Sea and River Water Analysis

The parameters that determine the corrosivity of the solution in this study are pH and salinity. Based on Table 1, the pH of seawater was 7.2, which refers to neutrality varies, while the pH of river water recorded was 6.3. Therefore, the pH of river water from Sungai Panchor, Muar, is slightly lower than that of seawater of Pontian, Johor, since the pH differences depend on human activities nearby, such as small business industries, food stalls, and human wastes [6]. Nitonye et al. [7] mentioned that low pH acid solution will accelerate corrosion by supplying hydrogen ions to the corrosion process.

Next, the natural seawater from Pontian, Johor has a higher salinity, which was 22.0 ppt, compared to the salinity of river water which was 0.4 ppt, as shown in Table 1. The salinity reading comprehends the amount of salt contained in that solution. Prifiharni et al. [8] point out that the higher the salt content is, the higher the corrosion rate due to the solution's increased electrical conductivity, which facilitates the cathodic reaction (oxygen reduction) and anodic reaction (iron dissolution). The increased amount of oxygen reaching the surface increases the rate of corrosion. Consequently, higher salinity greatly impacts the corrosion of the external surface of the X70 pipeline after periods of immersion.

Table 1: A measurement of pH and salinity for seawater and river water.

	Sampling Site	pH, ±0.1	Salinity, ppt
Seawater	Tambak Pontian, Johor	7.2	22.0
River water	Sungai Panchor, Johor	6.3	0.4

3.2 Weight Loss and Corrosion Rate Analysis

The X70 pipeline specimen immersed in river water indicated a higher weight loss compared to the X70 pipeline specimen immersed in seawater along with the period of immersion, which takes place for 7, 14, and 21 days, as shown in Figure 2. The average amount of mass lost by X70 steels after being immersed in seawater for 7, 14, and 21 days was 0.1097 g, while the loss of mass in river water was 0.0610 g. These results match those observed in earlier studies, which stated that the attack on steel immersed in seawater and river water is a function of the availability of dissolved oxygen at the metal-water interface that leads to the degradation of the steel surface [7].

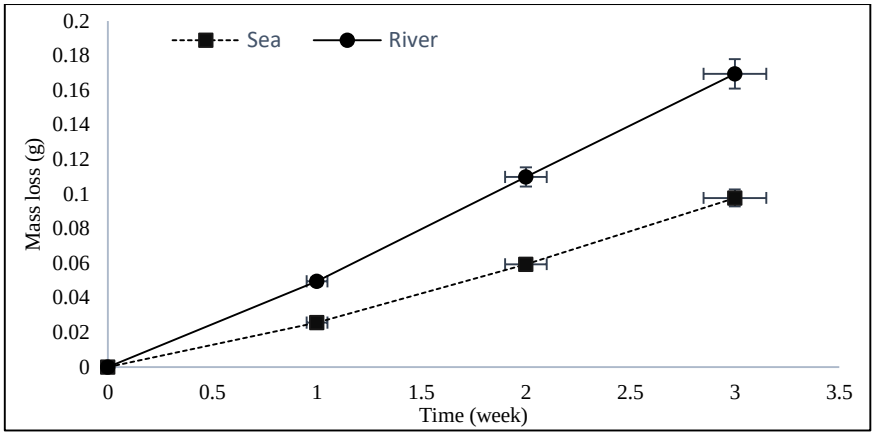

Figure 2: The variation of weight loss with time (weeks) of corrosion of the external surface of the X70 pipeline in seawater and river water.

Furthermore, the corrosion rate for X70 steel immersed in river water was higher compared to the corrosion rate for X70 steel immersed in seawater, as shown in Figure 3. This may be a consequence of the level of pH of river water being slightly acidic compared to seawater; as mentioned by Nitonye et al. [7], acidic waters with a low pH accelerate corrosion by contributing hydrogen ions to the process. Additionally, this finding was also reported by Mardhiah et al. [9], where the corrosion rate of carbon steel will be higher at a lower pH level solution. However, an increasing trend in the corrosion rate of X70 steel in seawater was observed. A possible explanation for this might be that when the salinity of the water increases, the water becomes more corrosive and accelerates the corrosion of pipeline steel [6]. Thus, both seawater and river water environments led to corrosion and effectively acted as a corrosive medium on X70 steel because both showed an increased trend in corrosion rate as a function of time.

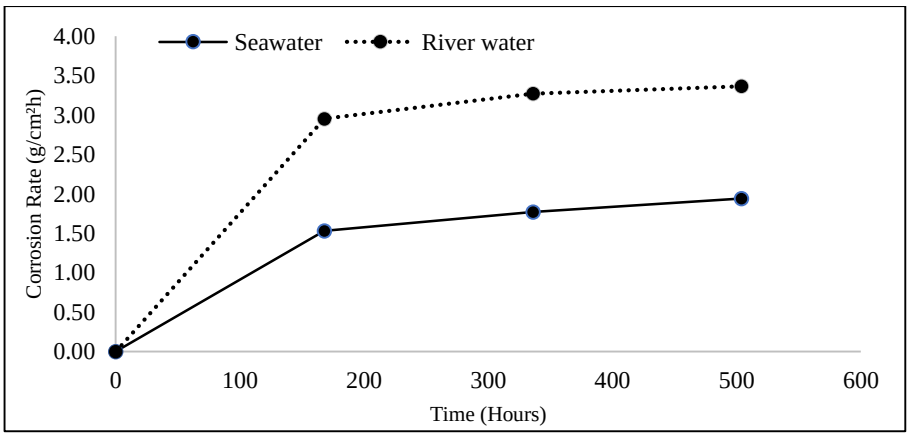

Figure 3: Corrosion rate of X70 steel sample after 7, 14, and 21 days of immersion in seawater and river water.

3.3 Observation On the Surface of External X70 Steel After Immersion Test Using DSX100 Opto-Digital Microscope

Figure 4 depicts the formation of an orange-colored corrosion product film on the surface of the sample that was observed using a DSX100 Opto-Digital Microscope. After 7, 14, and 21 days of immersion, the X70 steel sample was completely coated with a thick orange layer, proving the presence of corrosion products. A prior study conducted by Azam et al. [6] mentioned that iron hydroxide (Fe_xOH_y) and iron oxide (Fe_xO_y) might be the consistent corrosion products on the pipe's surface as the thick orange color was observed on the steel surface using an optical microscope. Additionally, this finding was also reported by Prifiharni et al. [8], where the formation of rust, which is the corrosion

product over the X70 steel, is due to the dissolution mechanisms of steel when immersed in an aggressive medium.

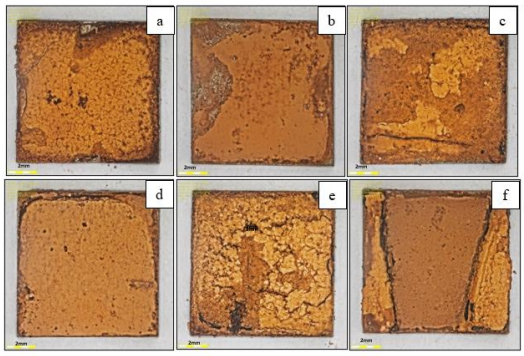

Figure 4: The optical image of sample surface changes after immersion in seawater for (a) 7 days (b) 14 days (c) 21 days, while that in river water for (d) 7 days (e) 14 days (f) 21 days.

3.4 X-Ray Diffraction (XRD) Analysis for Pre and Post-Immersion of X70 Pipeline Steel Sample

The XRD pattern for pre-immersion showed the sharp reflex at $2\theta = 44.60$ belongs to Fe, which is related to the specimen (X70). This result indicates the absence of a corrosion mechanism before immersion of the sample. The experimental XRD pattern for 7 days of immersion that is illustrated in Figure 5 (a) demonstrates the XRD pattern of amorphous oxide and low-intensive crystal phase on the X70 sample as corrosion products. The crystal formation of corrosion products is identified and mainly contributed by lepidocrocite, goethite, and hematite phase for seawater condition, while that in river water condition showed an intense peak of akageneite. In accordance with the present result, a previous study carried out by Jafery et al. [10] demonstrated that the presence of corrosion products of X70 steel occurred in the availability of oxygen and the migration of metal ions, Fe^{2+}, in the solution will accelerate the corrosion process.

Next, the XRD pattern for 14 days of immersion illustrated in Figure 5 (b) revealed the crystal formation of corrosion products in seawater consisting of lepidocrocite, goethite, and magnetite, while that in river water contained akageneite and new formation of crystalline phases such as lepidocrocite and magnetite. Xiao et al. [11], mentioned that akageneite is generally found with lepidocrocite in the outermost corrosion layer and existed in the inner rust layer associated with the existence of cracks. Then, the XRD pattern for 21 days of immersion in sea and river water illustrated in Figure 5 (c) displayed the same crystalline phase of corrosion products for 14 days. However, the intensity of the peaks decreases slightly with time. The finding was consistent with that of Kratzig et al. [12], who found in the studies that the crystalline phase of corrosion product ascended significantly with increasing time, presented by the higher number and smaller full-width half-maximum (FWHM) of the detected peaks.

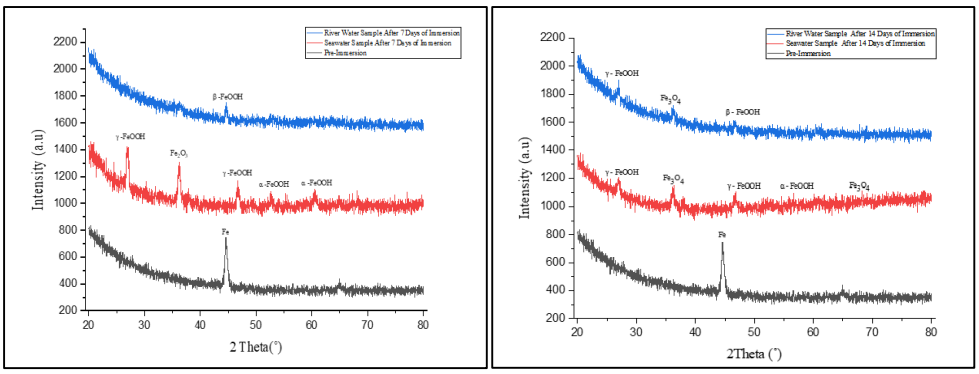

(a) (b)

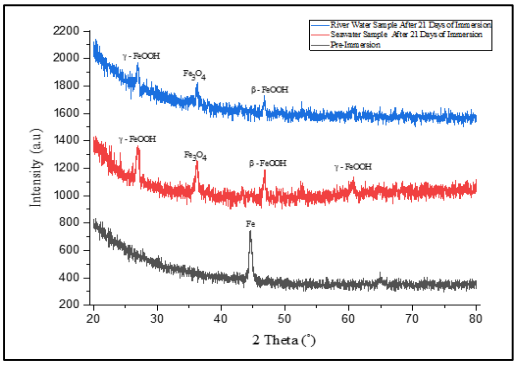

(c)

Figure 5: XRD pattern for X70 steel sample for pre and post-immersion in seawater and river water for (a) 7 days (b) 14 days (c) 21 days.

3.5 Field Emission Scanning Electron Microscopy (FESEM) Analysis

The surface morphology of the corrosion products formed on X70 steel for pre- and post-immersion are shown in Figure 6 (a-g). Surface morphology for pre-corrosion of X70 illustrated in Figure 6 (a) portrayed the non-homogenous surface that related with the findings by Omale et al. [13], where the non-homogenous surface of X70 pipeline consists of polygonal ferrite, bainite, and fine acicular ferrite grains. The micrograph of post-corrosion of the X70 sample in seawater for seven days displayed in Figure 6 (b) comprised the formation of a denser oxide layer that represents magnetite and revealed a sandy grain of lepidocrocite, while that in river water showed in Figure 6 (c) presented the sandy grain of lepidocrocite and the formation of cotton ball is identified as goethite.

Furthermore, the corrosion products that formed on the external surface of X70 after 14 days of immersion in seawater presented in Figure 6 (d) are identified as sandy grain and cracks lepidocrocite, while that in river water displayed in Figure 6 (e) proved the existence of corrosion products morphology such as oxide layer magnetite, and whiskers goethite. Lastly, post-corrosion of X70 in seawater after 21 days, illustrated in Figure 6 (f), showed the consistent observation of the morphological evolution of the corrosion products such as sandy grain lepidocrocite and the addition of bird's nest that also represents lepidocrocite, whilst in river water portrayed in Figure 6 (g) presents the corrosion products morphology including bird's nest lepidocrocite and dark layer magnetite. These findings are consistent with earlier research by Fonna et al. [14], which tabulated the morphology of the corrosion products. In those studies, lepidocrocite was indicated by sandy grains, cracks, and bird's nests, while goethite and magnetite were indicated by cotton ball and whisker morphologies and oxide layer, respectively.

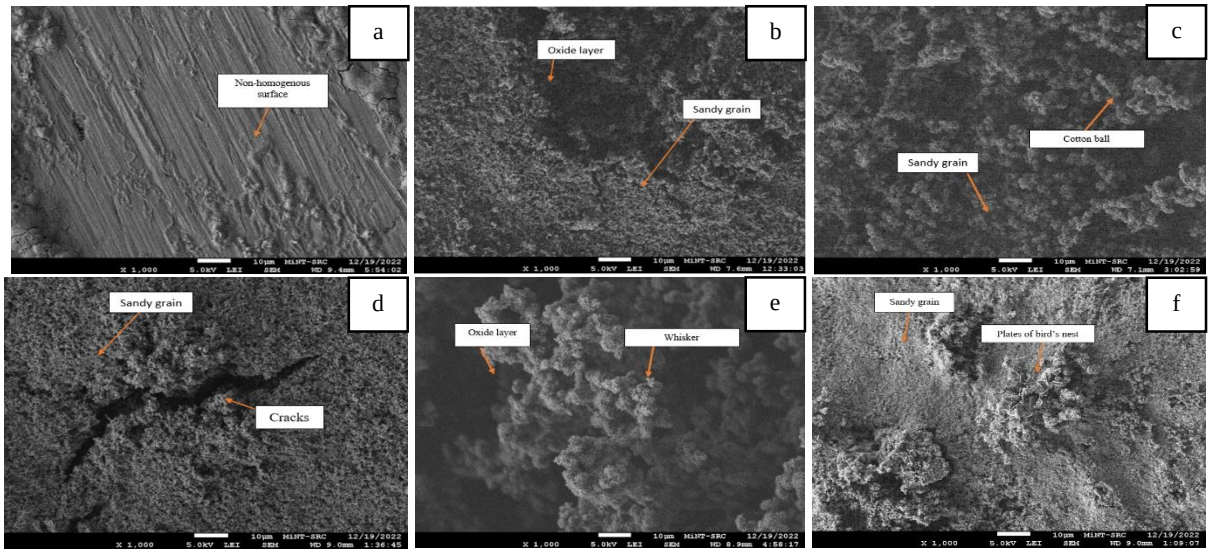

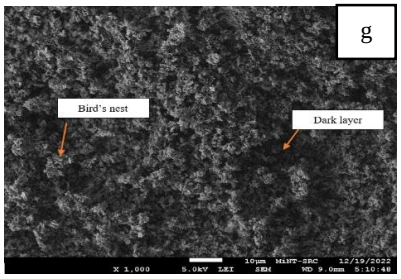

Figure 6: FESEM micrograph of X70 steel sample for pre and post-immersion (a)pre-immersion (b) 7 days in seawater (c) 7 days in river water (d) 14 days in seawater (e) 14 days in river water (f) 21 days in seawater (g) 21 days in river water.

3.6 Scanning Electron Microscopy with Energy Dispersive X-ray (SEM-EDX) Analysis for Pre- and Post-Immersion of X70 Pipeline Steel

SEM-EDX of corrosion products for X70 pipeline steel samples under all exposure circumstances is shown in Figures 7–9. Figure 7 (a) represents the pre-immersion X70 sample and illustrates a non-homogenous surface morphology. In accordance with previous studies by Omale et al. [13], the non-homogenous surface of the X70 pipeline is composed of polygonal ferrite, bainite, and fine acicular ferrite grains. Subsequently, EDX analysis in Figure 7 (b) outlined the elemental composition for pre-corrosion of X70, which contains mostly Fe (98.37%) and Si (1.63%). However, the presence of silicon elements found in the sample is due to the action of polishing the sample surface using 800-grit sandpaper.

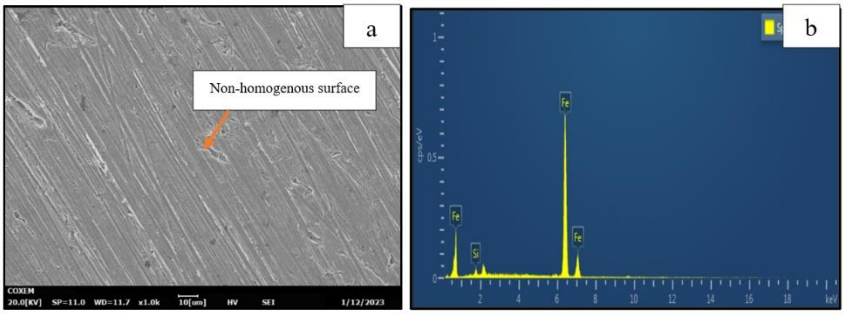

Figure 7: The surface morphology and elemental analysis of pre-immersion of X70 pipeline steel (a) SEM images (b) EDX spectrum.

Figure 8 (a) is an SEM image of the X70 pipeline after corrosion in seawater. It shows the shape of corrosion products like bird's nest lepidocrocite and cotton ball goethite. The EDX spectrum in Figure 8 (b) shows that X70 pipeline steel corrosion products contain Fe (74.54%) and O (24.04%). However, other elements were found in the sample, which was chlorine (Cl; 1.35%) elements. The possible explanation for this finding may be due to the presence of chloride content in seawater, which is supported by the fact that the seawater used in this study recorded a salinity reading of 22.0 ppt. In addition, the presence of chloride ions may induce a corrosion mechanism in X70 steel, as described by Chu et al. [15], where chloride ions in an aqueous solution may damage the passivation coating of steel by competing with hydrogen and oxygen ions during the adsorption process, thereby increasing the susceptibility of steel to corrosion.

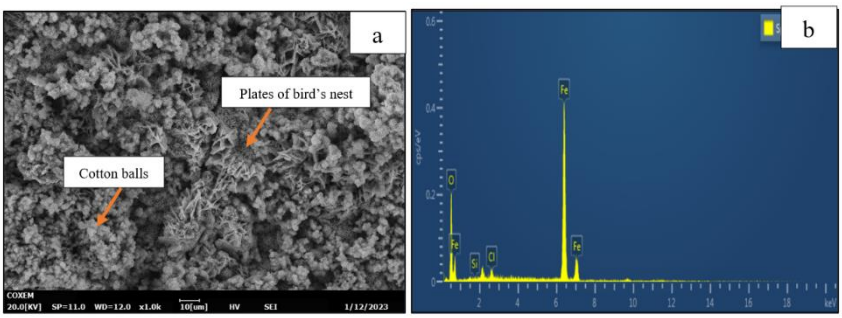

Figure 8: The surface morphology and elemental analysis of immersion of X70 pipeline steel in seawater for 21 days (a) SEM images (b) EDX spectrum.

Next, the SEM image depicted in Figure 9 (a) indicates sandy grain lepidocrocite and circular grain magnetite as the corrosion product morphology for post-corrosion of X70 pipeline steel immersed in river water. Apparently, more complex damage occurred on steel surfaces compared to the pre-immersion of X70 steel. Additionally, Jafery et al.[16], mentioned that the presence of sandy grain lepidocrocite may result in the formation of irregular amorphous corrosion products, whereas based on the study by Fuente et al. [17], the circular grain magnetite corrosion products are formed when the dissolved ferric species of FeOOH rust react with ferrous species in the solution. The elemental composition of the corrosion product observed in Figure 9(b) shows chemical composition diversity for Fe (74.44%), O (24.08%), and Cl (0.10%). Chlorine components in the EDX spectrum may be a result of river water contents, as the salinity of river water used in this study is 0.4 ppt. Therefore, it can be assumed that most corrosion products are made of iron oxides and iron hydroxides.

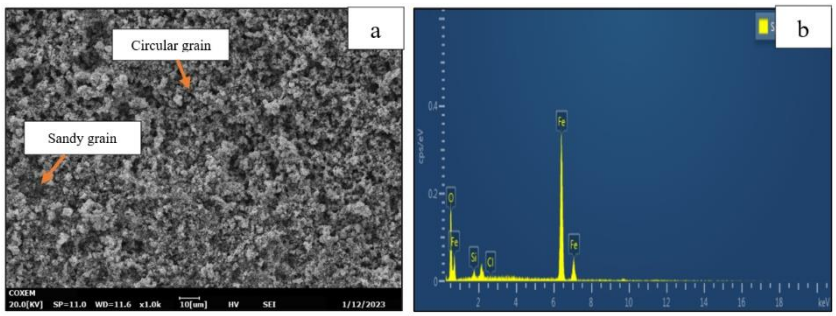

Figure 9: The surface morphology and elemental analysis of immersion of X70 pipeline steel in river water for 21 days (a) SEM images (b) EDX spectrum.

4. Conclusion

As a conclusion, several points can be summarized as follows:

i. The physical and chemical properties of sea and river water, namely pH and salinity, have a massive impact on the corrosion mechanism. The pH values were 7.2 for seawater and 6.3 for river water, and the salinity of seawater was 22.0 ppt, and that of river water was 0.4 ppt.
ii. The average mass loss of X70 steels immersed in sea and river water for 7, 14, and 21 days was 0.1097 g and 0.0610 g, respectively, proving that the external surface of X70 steel deteriorated more in river water compared to seawater. Therefore, the corrosion rate of X70 in river water was higher than that in seawater, as the average corrosion rate of those steels in river water was 3.1954 g/cm^{2}h, while that in seawater was 1.7470 g/cm^{2}h.
iii. The corrosion products formed on the X70 external steel surface become increasingly severe throughout the immersion in sea and river water. FESEM and SEM results show the formation of corrosion products, such as a thicker oxide layer, sandy grain, cotton ball, circular grain, cracks, bird's nest, and whiskers that represent lepidocrocite, goethite, and magnetite, whereas

pre-corrosion of X70 steel shows a non-homogeneous surface morphology. For EDX analysis, the main element composition of the corrosion product is Fe and O.

iv. The XRD analysis revealed the low-intense crystalline phases of the post-corrosion product that represent lepidocrocite (γ-FeOOH), goethite (α-FeOOH), hematite (Fe_2O_3), magnetite (Fe_3O_4), and akageneite (β-FeOOH), whereas the XRD analysis for pre-corrosion displayed a high-intense peak of Fe.

Acknowledgment

The authors would like to thank the Faculty of Applied Sciences and Technology, Universiti Tun Hussein Onn Malaysia, for its support in completing this project.

References

[1] International Energy Agency (IEA), "The Oil and Gas Industry in Energy Transitions," *Oil Gas Ind. Energy Transitions*, 2020.

[2] T. M. Ike, O. Adedipe, M. S. Abolarin, and S. A. Lawal, "Mechanical Characterization of Welded API X70 Steel Exposed to Air and Seawater: A review," *IOP Conf. Ser. Mater. Sci. Eng.*, vol. 413, no. 1, 2018,

[3] M. Wasim and M. B. Djukic, "Journal of Natural Gas Science and Engineering External corrosion of oil and gas pipelines : A review of failure mechanisms and predictive preventions Canadian Association of Petroleum Producers The National Association of Corrosion Engineers," *J. Nat. Gas Sci. Eng.*, vol. 100, no. November 2021, p. 104467, 2022,

[4] M. Lavaleye *et al.*, "Deep Corrosion On Site," pp. 16–43, 2014.

[5] G. Up, "The Effects and Economic Impact of Corrosion," *Corros. Underst. Basics*, pp. 1–20, 2019,

[6] M. A. Azam, S. Sukarti, and M. Zaimi, "Corrosion behavior of API-5L-X42 petroleum/natural gas pipeline steel in South China Sea and Strait of Melaka seawaters," *Eng. Fail. Anal.*, vol. 115, no. June, pp. 1–8, 2020,

[7] S. Nitonye, U. O. Emmanuel, and A. O. Ezenwa, "Combating Corrosion in Transmission Pipelines in Marine Environment Using Vernomia Amydalina as Inhibitor," *Open J. Mar. Sci.*, vol. 08, no. 04, pp. 450–472, 2018,

[8] S. Prifiharni, L. Nuraini, G. Priyotomo, Sundjono, H. Gunawan, and I. Purawiardi, "Corrosion performance of steel and galvanized steel in Karangsong and Limbangan sea water environment," *AIP Conf. Proc.*, vol. 1964, no. May, 2018,

[9] R. A. S. A. Mardhiah I, Norharzilan Y, Abdulhah A, Rasol, R, "Effect of pH corrosion sulphate reducing Mardhiah 2014.pdf," *Journal of environmental science and technology*. pp. 209–217, 2014.

[10] K. M. Jafery, Z. Embong, N. K. Othman, N. Yaakob, M. Shah, and N. Z. Nor Hashim, "Initial stage of corrosion formation for X70 pipeline external surface in acidic soil (peat) environment," *Mater. Today Proc.*, vol. 51, no. xxxx, pp. 1381–1387, 2021,

[11] H. Xiao, W. Ye, X. Song, Y. Ma, and Y. Li, "Evolution of akaganeite in rust layers formed on steel submitted to wet/dry cyclic tests," *Materials (Basel).*, vol. 10, no. 11, pp. 1–14, 2017,

[12] A. Kratzig, L. Q. Hoa, D. Bettge, M. Menneken, and R. Bäßler, "Early stage of corrosion formation on pipeline steel X70 under oxyfuel atmosphere at low temperature," *Processes*, vol. 8, no. 4, 2020,

[13] J. I. Omale, E. G. Ohaeri, A. A. Tiamiyu, M. Eskandari, K. M. Mostafijur, and J. A. Szpunar,

"Microstructure, texture evolution and mechanical properties of X70 pipeline steel after different thermomechanical treatments," *Mater. Sci. Eng. A*, vol. 703, no. July, pp. 477–485, 2017,

[14] S. Fonna, I. Bin M. Ibrahim, Gunawarman, S. Huzni, M. Ikhsan, and S. Thalib, "Investigation of corrosion products formed on the surface of carbon steel exposed in Banda Aceh's atmosphere," *Heliyon*, vol. 7, no. 4, p. e06608, 2021,

[15] X. Chu, M. Qing, and Y. Wang, "Effect of chloride ion on metal corrosion behavior under pinhole defect of coating studied by wbe technology," *Corros. Prot.*, vol. 40, no. 1, pp. 23–27, 2019,

[16] K. M. Jafery, Z. Embong, N. K. Othman, N. Yaakob, M. Shah, and N. Z. N. Hashim, "SEM-EDX and AFM analysis for the surface corrosion morphology structure and roughness on embedded X70 external pipeline in acidic soil (peat) environment," *Mater. Today Proc.*, vol. 48, pp. 1929–1935, 2021,

[17] D. de la Fuente, J. Alcántara, B. Chico, I. Díaz, J. A. Jiménez, and M. Morcillo, "Characterisation of rust surfaces formed on mild steel exposed to marine atmospheres using XRD and SEM/Micro-Raman techniques," *Corros. Sci.*, vol. 110, pp. 253–264, 2016,